THE ASTROPHYSICAL JOURNAL, 441:786–799, 1995 March 10

OBSERVATIONS OF THE X-RAY NOVA GRO J0422+32. I. OUTBURST AND THE DECAY TO QUIESCENCE

PAUL J. CALLANAN, MICHAEL R. GARCIA, JEFFREY E. MCCLINTOCK, AND PING ZHAO
Center for Astrophysics, 60 Garden Street, Cambridge, MA 02138

RONALD A. REMILLARD
Center for Space Research, Massachusetts Institute of Technology, Cambridge, MA 02139

CHARLES D. BAILYN[1] AND JEROME A. OROSZ[1]
Department of Astronomy, Yale University, 260 Whitney Avenue, New Haven, CT 06511

B. ALAN HARMON
ES84, NASA/Marshall Space Flight Center, Huntsville, AL 35812

AND

WILLIAM S. PACIESAS
Department of Physics, University of Alabama in Huntsville, Huntsville, AL 35899
Received 1994 June 13; accepted 1994 September 12

ABSTRACT

We present optical photometry and spectroscopy and BATSE observations of the X-ray nova GRO J0422+32, obtained during outburst and its subsequent decay to quiescence. Although the X-ray and optical properties of GRO J0422+32 are broadly similar to those of other X-ray novae, it is unique in several respects. The unusually protracted decay to quiescence of the optical light curve has been punctuated by at least two minioutbursts of ∼4 mag. The BATSE and optical outbursts are each separated by ∼120 days. We find that the optical luminosity of GRO J0422+32 during the primary outburst is dominated by reprocessing of $E > 10$ keV X-rays. In contrast, the optical minioutbursts are most likely generated by an intrinsically bright disk rather than X-ray reprocessing: they do not appear to have any X-ray counterparts. Extremely broad (up to 6000 km s^{-1} FWZI) absorption lines have also been observed during both primary outbursts and minioutbursts. During the second minioutburst, Hα and Hβ emission was observed superposed on red-shifted absorption features. We find that the interoutburst light curve of GRO J0422+32 may be inconsistent with an accretion disk instability as the origin of the minioutbursts. Finally, a transient 5.1/10.2 hr modulation, which may be related to the orbital period, has been observed during roughly half of our observations. However, confirmation of the orbital period must await observations in quiescence.

Subject headings: accretion, accretion disks — novae, cataclysmic variables — stars: individual (GRO J0422+32) — X-rays: stars

1. INTRODUCTION

Low-mass X-ray binaries (LMXBs) are systems in which a neutron star or black hole accretes material from a low-mass ($M \leq 1\ M_\odot$) secondary (see Bhattacharya & van den Heuvel 1991). X-ray novae form a subset of LMXBs whose properties are characterized by dramatic increases in flux from X-ray (factors of $\sim 10^5$–10^7) to radio energies on timescales of days, with a subsequent decay to quiescence on timescales of months.

The study of X-ray novae has been of crucial importance to our understanding of X-ray binaries. While these transients are in outburst, their X-ray and optical properties are very similar to those of the persistently bright LMXBs, where the optical flux is dominated by the reprocessed emission from the X-ray–irradiated disk. In quiescence, however, the disk often fades to reveal the secondary star itself. This allows detailed photometric and spectroscopic measurements of the secondary to be made, otherwise impossible in the outburst state and in most of the persistently bright LMXBs. The detection of a deep ellipsoidal modulation and/or the "SU UMa" effect (e.g., Callanan & Charles 1991) constrains the mass ratio.

More precise constraints on the mass of the compact object have been derived from absorption-line radial velocity data from the secondary. Three X-ray novae have been identified for which firm lower limits of $\sim 3\ M_\odot$ exist for the mass of the compact object: A0620−00 (McClintock & Remillard 1986), V404 Cyg (Casares, Charles, & Naylor 1992), and Nova Muscae 1991 (Remillard, McClintock, & Bailyn 1992). These systems are regarded as strong black hole candidates.

The frequency of black hole candidates among X-ray novae appears to be remarkably high; nine out of the 13 optically identified systems are strong or probable black hole candidates (van Paradijs & McClintock 1995).

GRO J0422+32 (Nova Persei 1992) was first detected by the BATSE experiment on *GRO* on 1992 August 5 (Paciesas et al. 1992). Within 5 days it had brightened to 3 crabs (40–230 keV), and with a position determined to within 0°2 (Harmon et al. 1992), Castro-Tirado et al. (1993) identified the transient with a star of B magnitude ~ 13.5. Both the X-ray and optical properties of GRO J0422+32 were at that stage very similar to those of well-studied black hole X-ray novae, and we embarked on a campaign of systematic monitoring of the decay light curve, as

[1] Visiting Astronomer, Kitt Peak National Observatory, NOAO, operated by the Association of Universities for Research in Astronomy (AURA), Inc., under cooperative agreement with the National Science Foundation.

well as a series of more intensive runs to study the short-term photometric and spectral behavior of GRO J0422+32.

The plan of this paper is as follows. In § 2 we outline our extensive photometry and spectroscopy observations. In § 3 we discuss the results of these observations in detail, including our long-term light curve and our attempts to determine the orbital period. In § 4 we discuss the nature of both the primary and secondary outbursts and the similarity of the latter to the outbursts of dwarf novae.

2. OBSERVATIONS

2.1. *Photometry*

Our long-term monitoring campaign was carried out with the cooperation of observers at the Whipple Observatory 1.2 m telescope on Mount Hopkins, starting 1992 November 18. An image was initially obtained every one or two nights. In addition, a sequence of more concentrated observations were carried out in an attempt to determine the orbital period. Most of this photometry was also performed using the 1.2 m on Mount Hopkins, with additional data obtained from the 1.3 m McGraw-Hill telescope at the Michigan-Dartmouth-MIT (MDM) Observatory and the 2.1 m at KPNO. See Table 1 for a detailed observing log, and Figure 1 (Plate 19) for a finding chart for GRO J0422+32 (obtained ~500 days after outburst).

All the CCD images were reduced using IRAF. DAOPHOT was then used to perform the relative photometry (except for the 1993 December data set, where aperture photometry was used). Profile fitting was especially important when GRO J0422+32 was relatively faint ($R \sim 19$), because of the presence of an $R \sim 19.2$ star 5″ to the northeast (see Fig. 1). Photometry was performed relative to stars A, B, and C marked on Figure 1, whose V and R magnitudes are listed in Table 2.

We plot in Figure 2 the long-term light curve of GRO J0422+32. We include data reported by other authors (see Zhao et al. 1994 for further details) to augment the coverage of the light curve. The epochs at which more intensive photometry were carried out are indicated (see Table 1 and Fig. 2). In Figures 3*a*–3*f* we show the light curves and Fourier transforms derived from these observations (where the ordinate for the latter is in units of one-fourth of the semiamplitude squared). For those data sets displaying significant nightly trends in the overall light curve (1993 October and December and 1994 January), each night was detrended with a linear fit to the data, before generating the Fourier transforms (and folded plots; see Fig. 4 and § 3.2).

TABLE 2

MAGNITUDES OF COMPARISON STARS[a]

Star	V	R
A......	14.15	13.65
B......	14.52	13.80
C......	15.67	15.06

NOTE.—Errors on these measurements are ±0.03.

[a] Stars are marked on Fig. 1.

2.2. *Spectroscopy*

The spectra presented here were obtained using the 1.3 m telescope at the MDM observatory; additional spectra were obtained using the KPNO 4 m telescope. All data were reduced using IRAF. The MDM spectra were obtained with the Mark III Spectrograph and the "TI 4849" CCD. A 3″1 slit and 600 line m^{-1} grating were used for the 5 Å resolution spectra, while a 300 line mm^{-1} grating was used for the 12 Å resolution spectra. The CCD and the spectrograph's optical elements create a drastic reduction in the sensitivity curve below 4000 Å, so no blocking filters are necessary for spectroscopy out to 7400 Å. Clouds on November 19 make the photometric accuracy of this spectrum uncertain, but for the remaining MDM data conditions were clear, and the internal photometric accuracy is ~10%. The KPNO data were obtained during minioutburst with the Ritchey-Chrétien spectrograph (time-resolved spectroscopy using the KPNO data will be examined in a future paper). A 2″ slit and the KPC-17B grating were used to obtain spectra with 4.4 Å resolution. Sky conditions were nonphotometric. The MDM and KPNO spectra are shown plotted in Figures 5*a*–5*d*, in approximate chronological order. Their epochs relative to the outburst light curve are indicated in Figure 2 (see Table 3 for further details).

2.3. *BATSE Observations*

BATSE monitored GRO J0422+32 through the outburst and subsequent decay using Earth occultations (Harmon et al. 1993). The source was observable in the 20–300 keV energy

TABLE 1

PHOTOMETRY LOG

Date	Magnitude	Telescope	Number of Exposures	Filter	Time Resolution (s)	Epoch of Outburst
1992 Oct 11–12..........	13.3	MDM	745	V	60	I
1992 Oct 14–15..........	13.3	Mount Hopkins	910	V	60	I
1992 Nov 18	13.6	MDM	461	V	60	II
1993 Jan 21, 22, 25	13.8	Mount Hopkins	182	R	80	III
1993 Oct 9, 11, 12	18.8	Mount Hopkins	109	R	600	IV
1993 Dec 13.............	14.9	KPNO 2.1 m	128	V	45–60	V
1993 Dec 13, 15	14.9	Mount Hopkins	297	R	180	V
1994 Jan 3–5, 9–12......	18.0	Mount Hopkins	345	R	400	VI

NOTE.—To determine the epoch of the observation relative to the phase of the outburst, see Fig. 2. Magnitudes are approximate means over the observation interval (see § 3.2). For those data taken in V, we added a 0.4 mag offset to correct to the R-band flux.

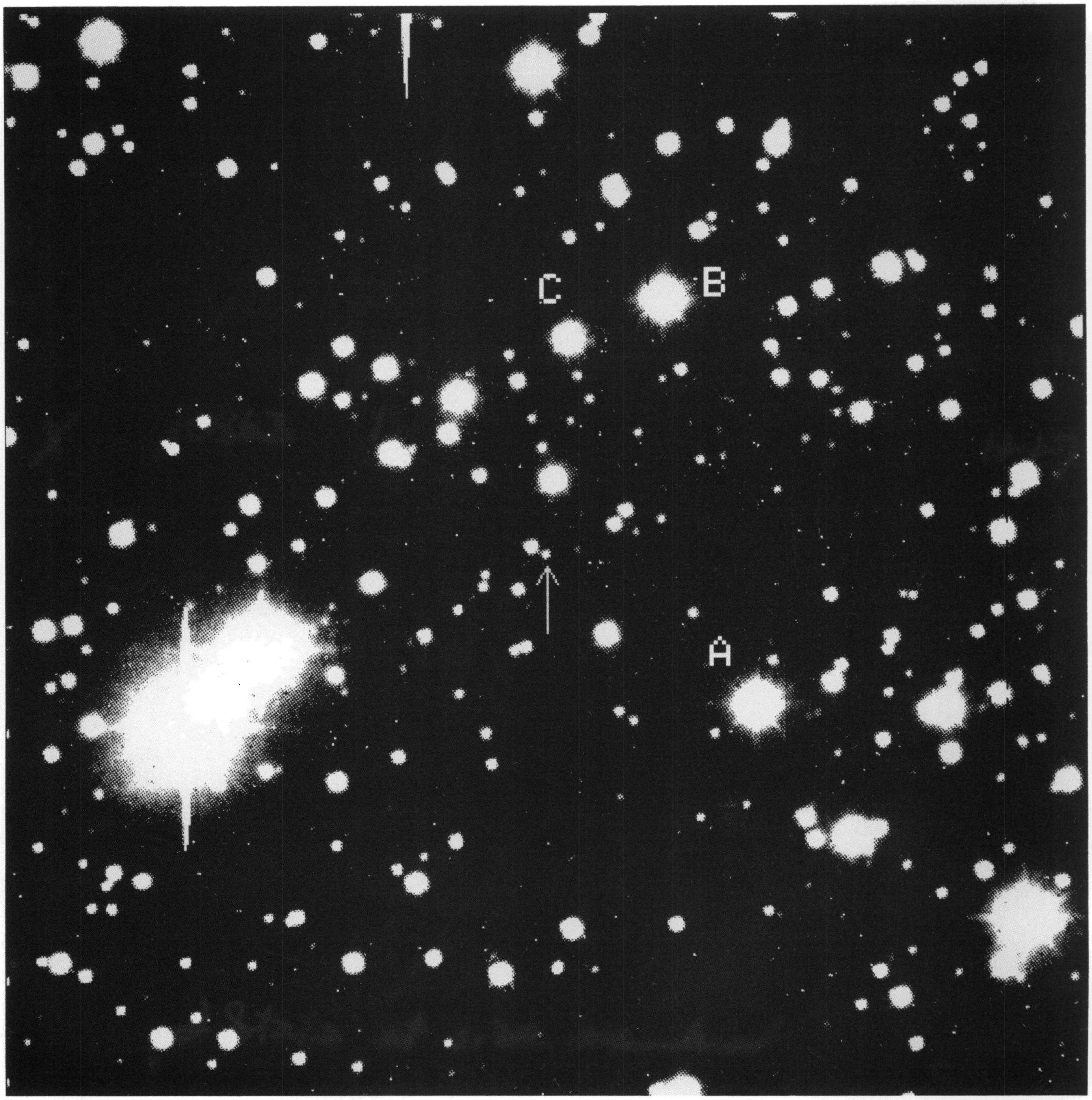

FIG. 1.—*R*-band 300 s image of GRO J0422+32. The field of view is 5′ × 5′ with north at the top and east to the left. GRO J0422+32 is indicated by an arrow. The magnitudes of stars A, B, and C are listed in Table 2.

CALLANAN et al. (see 441, 787)

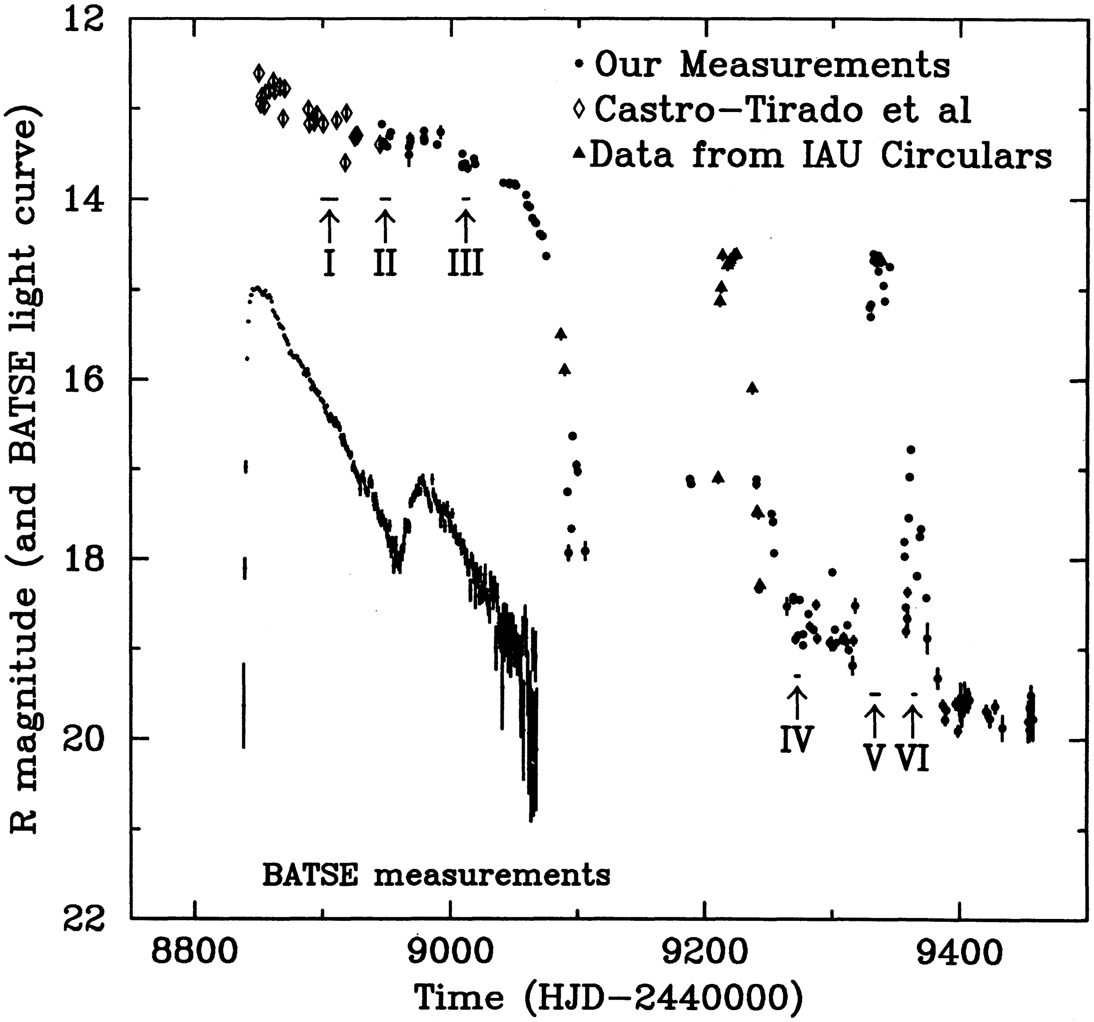

FIG. 2.—Outburst and decay light curve of GRO J0422+32. We have included the measurements of Castro-Tirado et al. (1993) and those reported in various IAU Circulars. Superposed are the epochs of more intensive observations discussed in the text. The length of each horizontal bar at each arrow denotes the approximate time base of the observations at that epoch. We also show the BATSE (20–300 keV) light curve, where the data have been scaled as $-2.5 \log$ (BATSE photons cm^{-2} s^{-1}) + 15, where the BATSE measurements are in the 20–300 keV band.

band for ~200 days after outburst, at which point it dropped below the BATSE sensitivity limit of 100 mcrab (3 σ; 1 day integration) and has remained below that level subsequently. In Figure 2 we show the BATSE data summed over 1 day intervals. Near the peak of the outburst, the statistical significance of each point is ~90 σ; however, we estimate that the errors are dominated by a systematic error of ~20%.

TABLE 3

SPECTROSCOPY LOG

Date	Telescope	Wavelength Range (Å)	Resolution	Epoch of Outburst
1992 Oct 6..........	MDM	3860–5200	5	I
1992 Oct 9..........	MDM	4050–5100	5	I
1992 Nov 19........	MDM	4300–7200	12	II
1992 Nov 21........	MDM	4300–7200	12	II
1992 Nov 24........	MDM	3860–5200	5	II
1993 Dec 8–10......	KPNO 4 m	4400–7000	4.4	V

NOTE.—Exposure times for the MDM observations varied between 20 and 70 minutes. Each KPNO spectrum is the sum of an entire night's exposure. The net exposure times are 3, 6, and 5 hr for December 8, 9, and 10 spectra, respectively. To determine the time of these observations relative to the epoch of the outburst, see Fig. 2.

3. RESULTS

3.1. *The Outburst and Long-Term Light Curve*

Study of a digitized image from the STScI "Quick *V*" survey shows nothing at the position of GRO J0422+32, to a limiting magnitude of $V \sim 19.5$. This is confirmed by examination of the POSS plates, yielding R(quiescent) ≥ 20. Taking R(maximum) ~ 12.6 (see Fig. 2) yields an amplitude for the optical outburst (hereafter the "primary" outburst) of ≥ 7.4 mag, comparable to that observed for other X-ray novae (e.g., van Paradijs & McClintock 1995).

Our BATSE light curve of GRO J0422+32, measured over the 20–300 keV energy range, is characterized by an *e*-folding time of 44 days (see Fig. 2), corresponding to ~0.05 "mag" day^{-1}. In contrast, the initial (as measured from day 10 to day 120 after outburst) rate of decay in the R band is only 0.0056 mag day^{-1}. This is a remarkably slow rate. For comparison, the decay rate of A0620−00 was 0.015 mag day^{-1} (Whelan et al. 1976), and for Nova Muscae 1991 it was 0.018 ± 0.002 mag

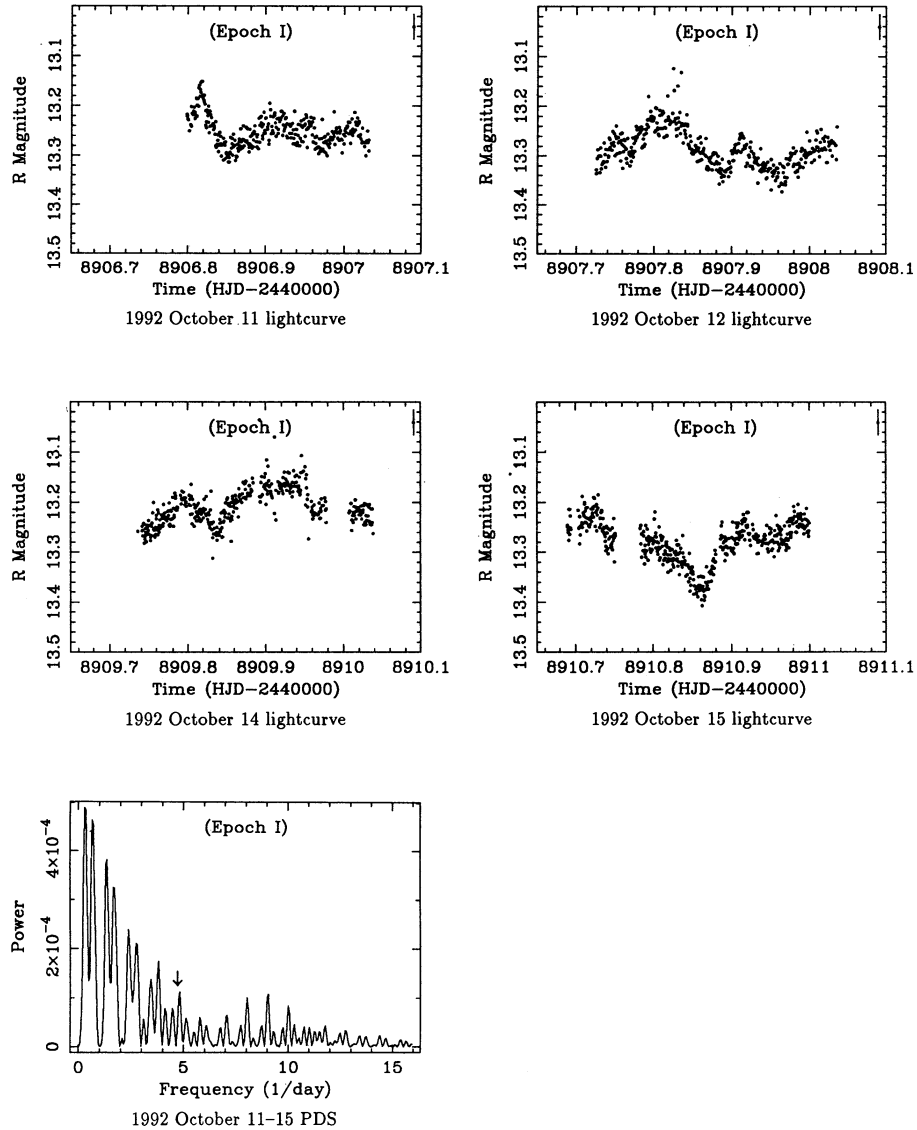

FIG. 3*a*

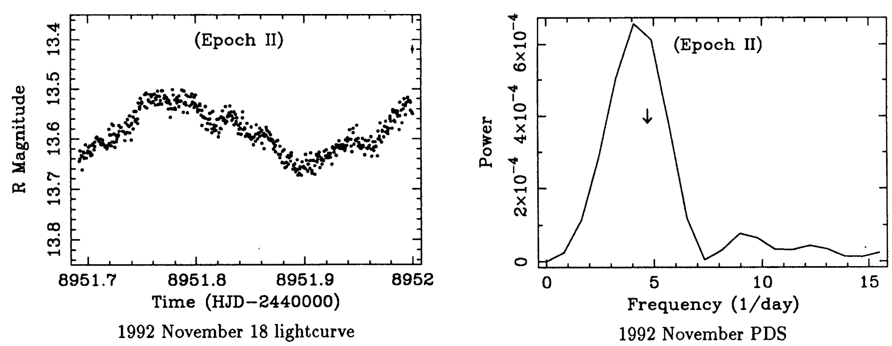

FIG. 3*b*

FIG. 3.—(*a*–*f*) Optical light curves of the more intensive observations. The epoch of the observations relative to the light curve in Fig. 2 is denoted in each graph. Representative error bars are plotted in the upper right-hand corner of each plot. Also shown are the Fourier transforms for each light curve, with the position of the 5.09 hr period marked.

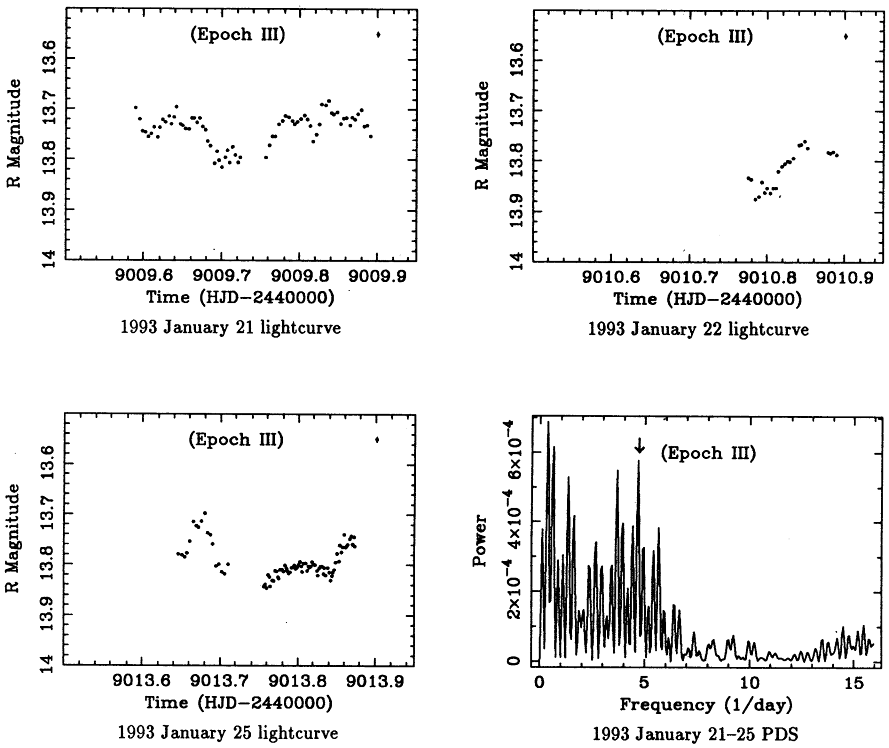
(Epoch III)
R Magnitude
Time (HJD−2440000)
1993 January 21 lightcurve
1993 January 22 lightcurve
1993 January 25 lightcurve
Power
Frequency (1/day)
1993 January 21–25 PDS

FIG. 3c

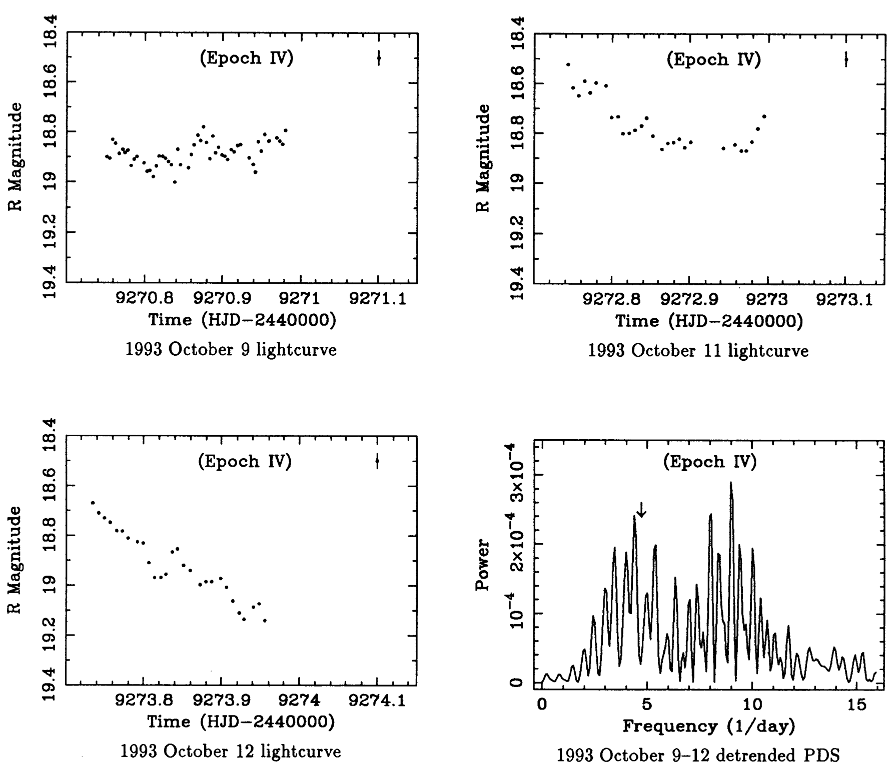
(Epoch IV)
R Magnitude
Time (HJD−2440000)
1993 October 9 lightcurve
1993 October 11 lightcurve
1993 October 12 lightcurve
Power
Frequency (1/day)
1993 October 9–12 detrended PDS

FIG. 3d

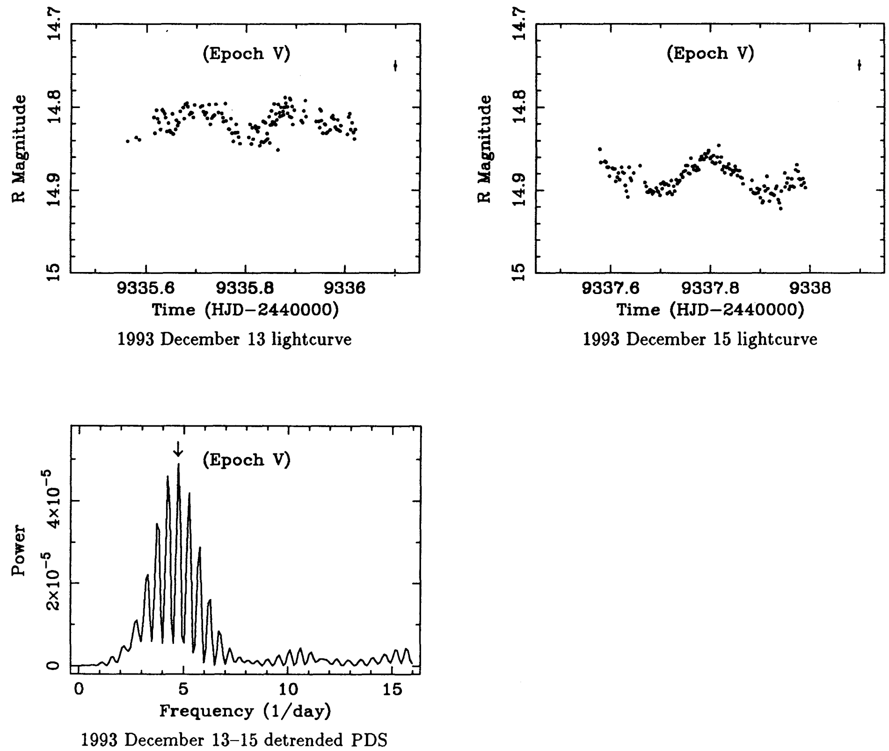
(Epoch V)
R Magnitude
Time (HJD−2440000)
1993 December 13 lightcurve
(Epoch V)
R Magnitude
Time (HJD−2440000)
1993 December 15 lightcurve
(Epoch V)
Power
Frequency (1/day)
1993 December 13–15 detrended PDS

FIG. 3*e*

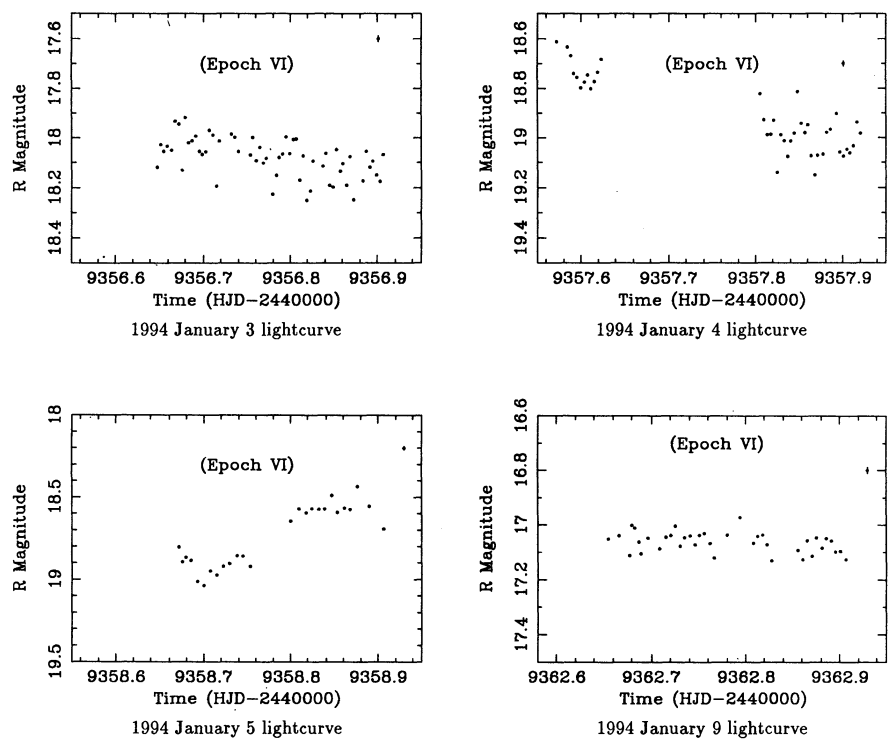
(Epoch VI)
R Magnitude
Time (HJD−2440000)
1994 January 3 lightcurve
(Epoch VI)
R Magnitude
Time (HJD−2440000)
1994 January 4 lightcurve
(Epoch VI)
R Magnitude
Time (HJD−2440000)
1994 January 5 lightcurve
(Epoch VI)
R Magnitude
Time (HJD−2440000)
1994 January 9 lightcurve

FIG. 3*f*

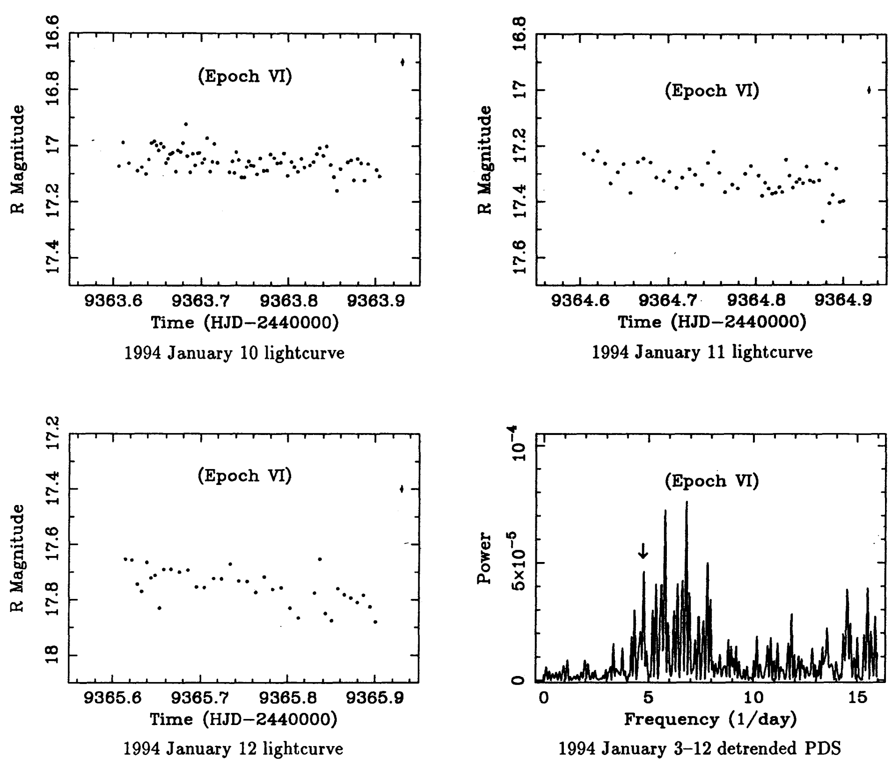

FIG. 3*f*—*Continued*

day^{-1} (Della Valle et al. 1991a; we have independently measured the decay rate from their Fig. 3). At about the time the X-rays dropped below the BATSE sensitivity limit, the optical light curve began a precipitous fall from $R \sim 14$ to $R \sim 18$ (day 120 to day 180 after outburst), at a mean rate of $\sim$0.09 mag day^{-1}. The mean $V-R$ during outburst was measured to be 0.4 ± 0.1. A significant reddening occurred during the decay, with $V-R = 1.3 \pm 0.25$ when the system reached $R \sim 20$.

In addition to the primary outburst, GRO J0422+32 has also exhibited at least two optical "minioutbursts," each of duration $\sim$20 days, reaching $R \sim 15$. Observation of this behavior is unprecedented among X-ray novae: we discuss it further below.

3.2. *The Search for the Orbital Period*

A modulation at 5.1 hr (or possibly 10.2 hr) in the light curve of GRO J0422+32 which may be orbital in nature has been reported by various authors (Chevalier & Ilovaisky 1992; Kato, Mineshige, & Hirata 1993, 1994). Indeed, Kato et al. detected a significant difference between the period observed $\sim$100 days after outburst and that observed $\sim$1 month later as GRO J0422+32 continued its decay to quiescence. From this they inferred a mass of the compact object in the range 3–6 $M_{\odot}$. However, the determination of the orbital period of an X-ray nova during *outbust* has proved notoriously unreliable. For example, in the case of V404 Cyg, 10 minutes or 5 hr were both suggested as possible orbital periods, before the true period of 6.4 days was finally determined from observations made in quiescence (see, for example, the review by Tanaka & Lewin 1995). Nevertheless, we have made a detailed search of our photometry for evidence for a 5.0906 ± 0.0005 hr period (the best estimate of Kato et al.). As Figures 3 and 4 show, we do find evidence for a transient 5.1/10.2 hr periodicity in our CCD photometry. In particular, note the following:

1992 October (*Epoch I*).— These data show no evidence for a coherent period at 5.1 hr, although considerable short-term variability is observed. Fourier analysis of the October light curve yields an upper limit on the semiamplitude of any periodic modulation of 0.03 mag (3 σ) for periods of 2–8 hr (see Fig. 3*a*). Folding the data on 10.18 hr produces a weakly detected modulation of semiamplitude $\sim$0.03 mag (see Fig. 4*a*).

1992 November (*Epoch II*).—Here a very significant 0.14 mag modulation is found (Fig. 3*b*). Because the data set is so short (only 7 hr), the period of the modulation is poorly constrained, and a 5.1 hr modulation would be consistent with the data.

1993 January (*Epoch III*).—A 5.12 ± 0.03 hr modulation was observed, with an amplitude of $\sim$0.1 mag (where the error in the period has been determined from measurements of the three dips observed in the data). This period is consistent with that discussed above. In Figure 4*b* we plot the data folded on this period. However, as the Fourier transform in Figure 3*c* shows, there are other peaks in the power spectrum of comparable significance.

1993 October (*Epoch IV*).—No 5.1 hr modulation was present in these data; we place an upper limit of 0.03 mag (3 σ) on the amplitude of any such modulation. A similar limit can be placed on the presence of any ellipsoidal modulation at half this period. It is more difficult to constrain the amplitude of a modulation at twice this period, because of the significant night-to-night variability of the data (see Figs. 3*d* and 4*c*).

1993 December (*Epoch V*).—We obtained photometry fortuitously close to the maximum of the second minioutburst.

1995ApJ...441..786C

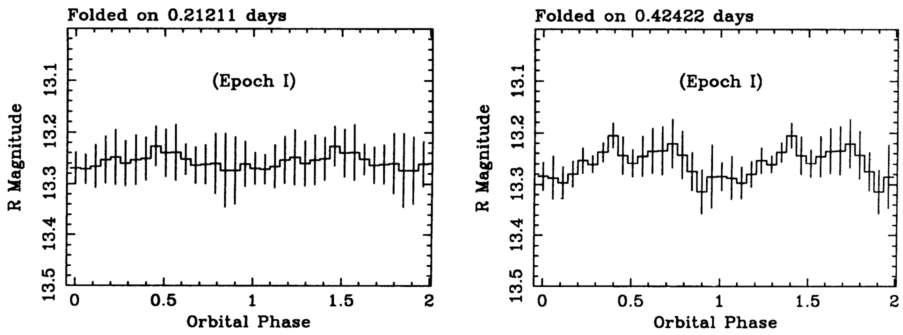

FIG. 4*a*

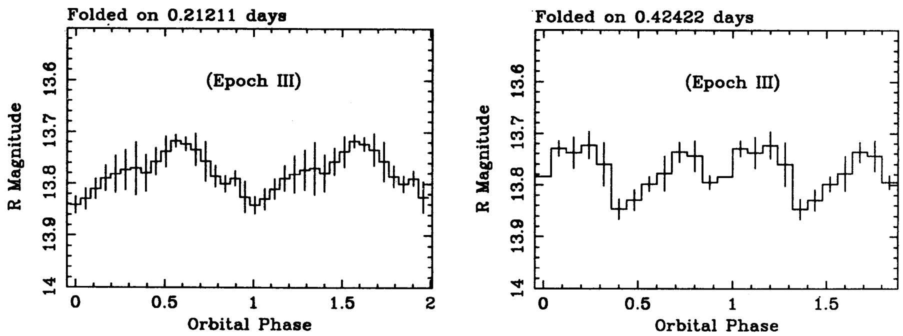

FIG. 4*b*

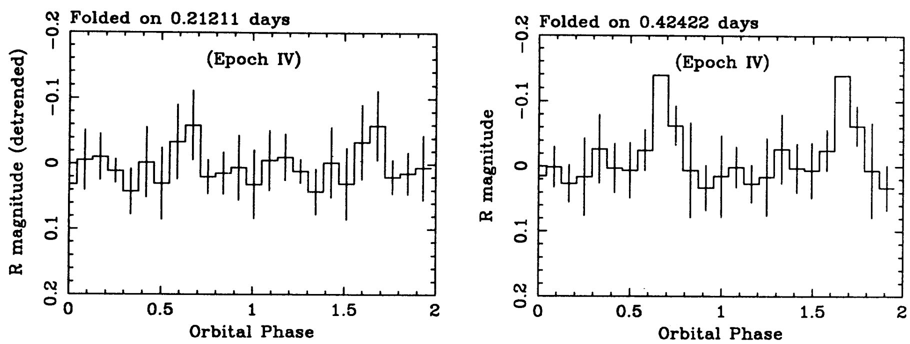

FIG. 4*c*

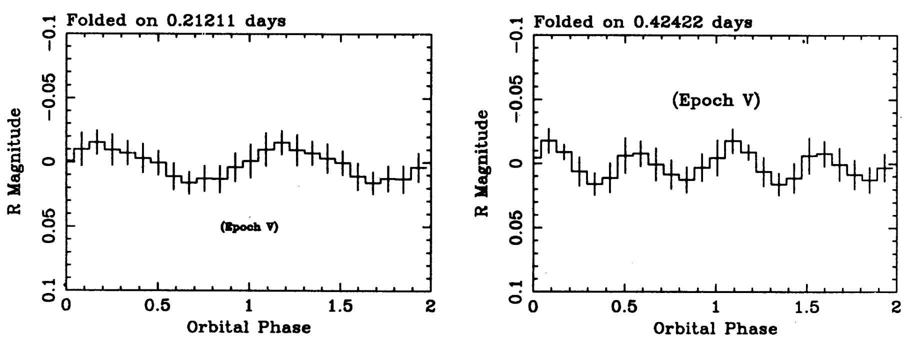

FIG. 4*d*

FIG. 4.—(*a–e*) Data of Fig. 3 folded on 5.09 and 10.18 hr. Because of the long-term variability of GRO J0422+32 during the 1993 October and December and 1994 January observations, each of these data sets has been detrended by subtracting a linear fit to the light curve of each night.

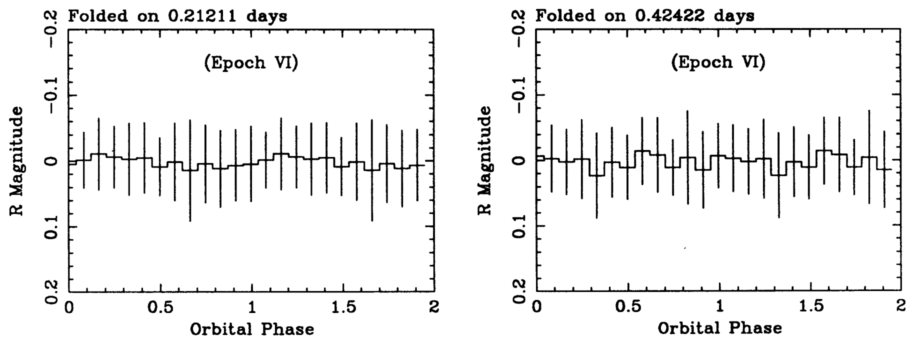

FIG. 4*e*

Here a ~5.055 ± 0.013 hr modulation returns to the light curve (see Figs 3*e* and 4*d*), with a semiamplitude of 0.025 mag (here the error in the period has been determined from a sine-wave fit to the data). Unfortunately, the short time base of our observations precludes the phasing of this modulation with that observed in 1993 January. The sinusoidal nature of this modulation is strongly reminiscent of an X-ray–heated secondary (e.g., van Paradijs 1983a); see, however, § 4.6.2.

1994 January (*Epoch VI*).—No clear modulation at 5.1/10.2 hr is present in this data set. We place an upper limit of 0.03 mag (3 σ) on the amplitude of any such modulation (see Figs. 3*f* and 4*e*).

We subdivided our entire data set into "high"-state (epochs I, II, III, and V) and "low"-state (epochs IV and VI) data and analyzed them independently. In Figure 6*a* we plot the Fourier transforms of these two data sets, where each night has been detrended by subtracting a linear fit to the data. The most powerful peak in the "high"-state data is at a period of 5.0486 ± 0.003 hr, with a semiamplitude of 0.028 mag. The error is conservatively estimated to be the distance to adjacent peaks (as plotted in Fig. 6*b*). There is also considerable power at the ±1 day aliases of these periods. In contrast, no clear modulation is apparent in the "low"-state data.

Note that our best estimate of the orbital period is apparently inconsistent with the period of Kato et al. (1994) (*arrow*). The source of this discrepancy lies in the epoch I and II data: these specifically are inconsistent with the Kato et al. period (for example, see Figs. 3*a* and 4*a*). On the other hand, the epoch III and V data sets (the 1993 "high"-state data) may be consistent, although these data are badly affected by aliasing (Fig. 6*c*). It is clear that the determination of the true orbital period must await the return of GRO J0422+32 to its quiescent state.

3.3. *Spectroscopy*

3.3.1. *The 12 Å Resolution Spectra*

Two spectra at a resolution of 12 Å were taken during epoch II, 3 months after the outburst and when GRO J0422+32 was still very bright (Fig. 5*a*). The spectra are similar to those of Nova Muscae 1991 a few days after outburst (e.g., Della Valle, Jarvis, & West 1991b). One notable difference is the weakness here of the N III Bowen fluorescence lines at 4640 Å, which were much stronger in earlier spectra of GRO J0422+32 (Shrader et al. 1993). The very blue continuum reddens slightly from November 19 to November 21, as the flux decreases. Interstellar lines due to the Na D doublet at ~5890 Å, the blend at 5778, 5780, and 5797 Å, and the blend at 6269 and 6283 Å are marked in Figure 5*a* (see Table 4B for further details). Emission lines also marked on the figure include Hα, Hβ, He II $\lambda\lambda$4686 and 5411, and He I $\lambda\lambda$5876 and 6678. The equivalent widths of the emission lines are only a few angstroms, as is typical of LMXBs in outburst (see Table 4A). The Hβ emission lines are embedded in broad absorption troughs.

3.3.2. *The 5 Å Resolution Spectra*

Three spectra at a resolution of 5 Å were also taken during epochs I and II (Fig. 5*b*). Some of the Hβ and He II λ4686 emission lines appear to be double peaked, with separations of 700–1000 km s^{-1}. Similar separations are seen in the double-peaked emission lines arising in the quiescent accretion disks of the black hole binaries Nova Muscae 1991 and A0620−00 (Orosz et al. 1994). All of the H Balmer lines visible in these spectra (Hβ–Hϵ) also show wide (3000 km s^{-1} FWZI) absorption. We note that as one goes toward the blue, the absorption lines remain strong relative to the emission lines. The continuum level decreases between 1992 October 6 and 9, but then increases by a factor of ~2 by November 24. The absorption lines of the higher Balmer series are particularly prominent at this higher flux level.

3.3.3. *The KPNO 4 m Spectra*

Each of the spectra presented in Figure 5*c* is the grand sum obtained during a single night's observation. The KPNO spectra were obtained at the maximum of the 1993 December minioutburst (at $R \sim 14.7$). As with the primary outburst spectra, the data obtained during December 8–10 show both Hα and Hβ in absorption, with emission-line cores. The FWZI of the absorption features is broad, ~6000 km s^{-1}. The Hβ asymmetric profiles (and possibly the Hα profiles too) are caused by redshifted absorption rather than blueshifted emission (see § 4.2 for more details).

There is clear evolution of the equivalent width of these line profiles with time (see Table 4A and Fig. 5*d*), with Hα in emission by December 10. This is accompanied by an increase in the He II λ4686 flux: the spectra also become marginally bluer. Note, however, that, even at the maximum of this mini-outburst, $B-V = 0.38 \pm 0.02$ (measured photometrically on 1993 December 13), considerably redder than during primary outburst ($B-V = 0.15$; Beskin et al. 1992).

4. DISCUSSION

4.1. *The Reddening and Distance to GRO J0422+32*

The reddening toward GRO J0422+32 can be estimated from the strength of the interstellar absorption lines. We used both our MDM and our KPNO spectra to measure the lines

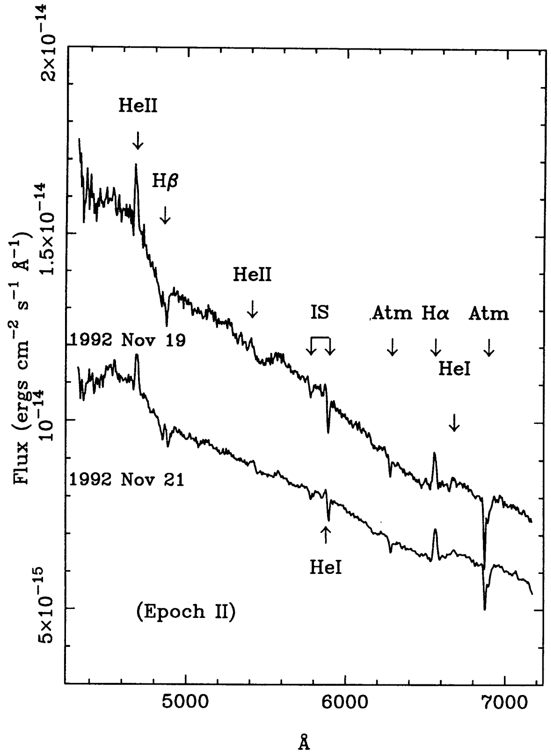

FIG. 5a

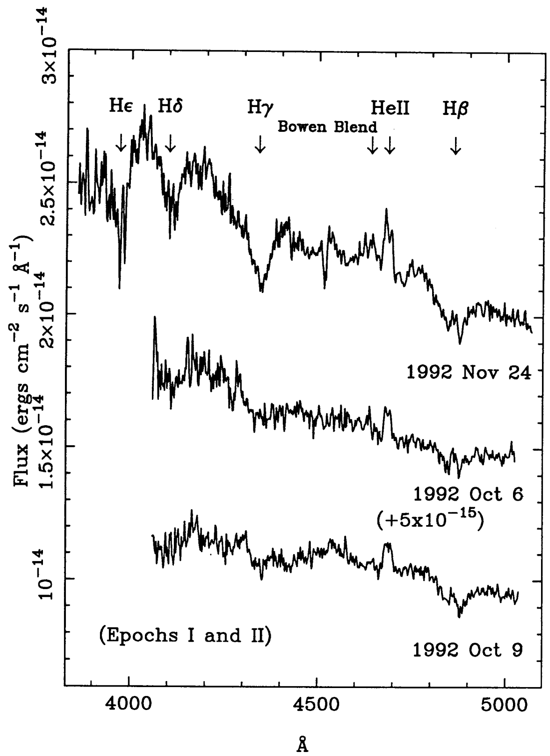

FIG. 5b

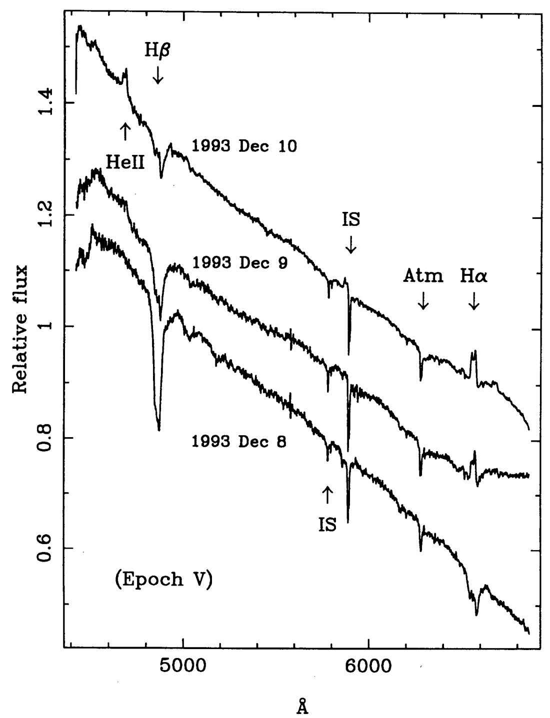

FIG. 5c

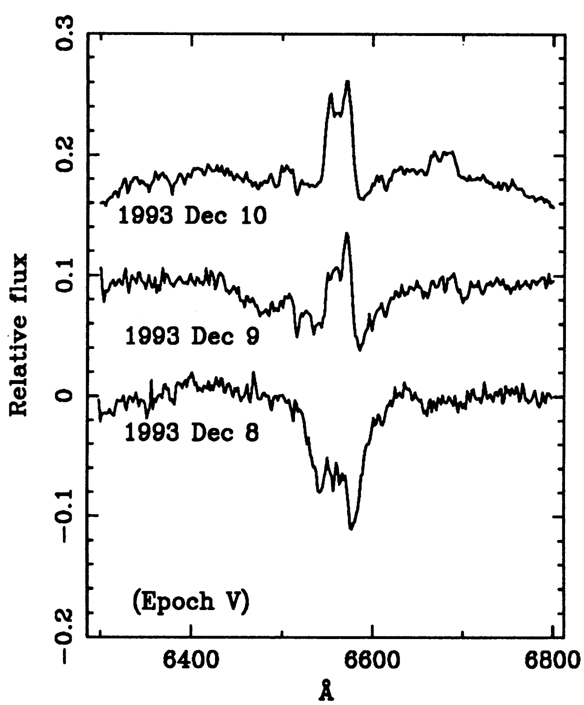

FIG. 5d

FIG. 5.—(*a*–*d*) MDM outburst spectra at 12 and 5 Å resolution and the KPNO 4 m spectra. Conditions for the MDM were generally photometric, but not so for the KPNO observations (see text for further details). The epochs of the observation (as shown in Fig. 2) are indicated. For (*d*) we have subtracted a linear fit to the local continuum of each spectrum, so that the evolution of the line profiles can be more easily compared. We have also plotted the best Gaussian fit to the Hβ absorption profiles, slightly displaced from the data for clarity. The vertical line represents the rest wavelength for Hβ. The scale of the Hα plot is such that the small shift between the absorption and emission features cannot be clearly discerned.

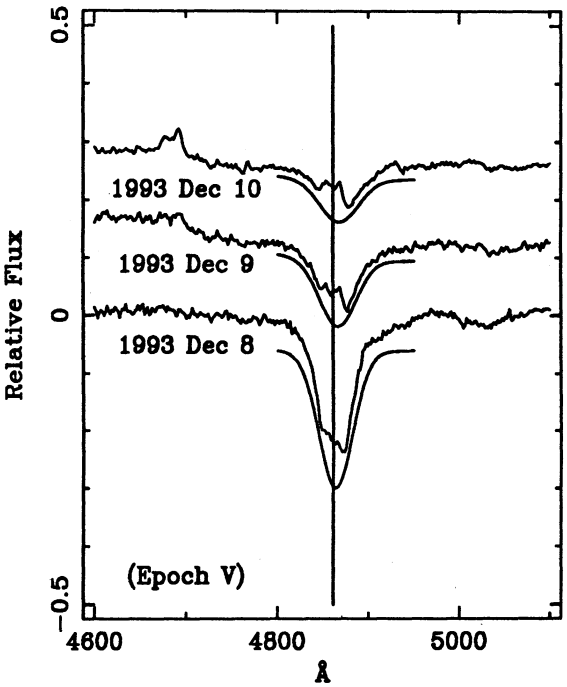

FIG. 5*d*—*Continued*

and obtained consistent results (Table 4B). The equivalent width of the Na D doublet at 5890 Å indicates $E(B-V) = 0.3 \pm 0.1$, where the error is dominated by the uncertainties in the function derived by Barbon et al. (1990) which relates the Na D width to $E(B-V)$. The equivalent width of the blend at 5778, 5780, and 5797 Å indicates $E(B-V) = 0.3 \pm 0.1$, where the error is again estimated from the uncertainties in the relation derived by Herbig (1975). The blend at 6269 and 6283 Å is most likely dominated by atmospheric (rather than interstellar) absorption. If assumed to be interstellar, it indicates an anomalously high absorption of $E(B-V) = 0.8 \pm 0.1$ from the relation of Herbig (1975). Note that these atmospheric features are listed as interstellar absorption lines in the spectra of GS 2000+25 in outburst (Charles et al. 1991) and Nova Muscae 1991 in outburst (Della Valle et al. 1991b); in both cases they would indicate an absorption much higher than that determined from other lines.

Our measurement of the interstellar lines therefore indicates $E(B-V) = 0.3 \pm 0.1$, which can be compared to the values measured by Shrader et al. (1993) of $E(B-V) = 0.2 \pm 0.1$ for the 5780 Å feature and $E(B-V) = 0.4 \pm 0.06$ for the 2200 Å feature.

These values correspond to a distance d in the Galactic plane of ~1–2 kpc (e.g., Allen 1973). However, even if $d \sim 1$ kpc, the Galactic latitude of GRO J0422+32 (−11°.9) is such that the source is clear of the Galactic reddening layer. Hence we can only place a lower limit of 1 kpc on the distance of GRO J0422+32 from extinction measurements alone.

4.2. *Origin of the Spectral Lines*

The wide, shallow Balmer absorption lines seen in GRO J0422+32 are an unusual feature for an X-ray nova in outburst. However, we note that the spectrum of Nova Muscae 1991 taken during outburst (Della Valle et al. 1991b) may show a similar feature at Hβ. Certainly such features have long been known in dwarf novae in outburst and have been ascribed to rotational broadening in the inner accretion disk (see the review by Warner 1976).

We have measured the redshift of the 1993 December absorption features by excluding the central emission-line cores and fitting Gaussian profiles to the wings. We fitted the profiles of the Hβ lines on all three nights, and Hα on December 8 only; the remaining Hα profiles are too strongly contaminated by the emission-line cores (Fig. 5*d*). We find redshifts of 240, 460, and 580 km s^{-1} for Hβ on the nights of December 8, 9, and 10, respectively, and 100 km s^{-1} for the Hα profile on December 8. The formal error on the measurement of the absorption-line centers is ~50 km s^{-1}. The Hα and Hβ emission-line profiles do not appear to be redshifted, and have velocities within ±100 km s^{-1} of zero (as determined by fits to the wings of the emission features). The MDM data also show redshifted absorption lines, with velocities consistent with the KPNO results, but the measurement errors are higher because of the poorer signal-to-noise ratio of these spectra. We briefly discuss three possible causes for such redshifts.

1. An asymmetry in the disk. Weak, blueshifted emission may distort the absorption-line profiles. Indeed, in *quiescence* such excess emission is intermittently present in the blue wing of the Hα line for both A0620−00 and Nova Muscae 1991 (Orosz et al. 1994).

2. A wind from the disk. Redshifted absorption arising from mass loss from the disk could give rise to redshifted profiles. However, we would also expect a corresponding blueshifted component, which is not observed. Note that the superposition of a P Cygni profile on a broad absorption line will produce an apparent blueshift, rather than a redshift of the line centroid.

3. More speculatively, the redshift could be gravitational in origin. If the primary in GRO J0422+32 is indeed a black hole, the required redshift could be generated by material located $\sim 2 \times 10^9$ cm from a 10 $M_\odot$ primary. The Keplerian velocity of this material would be ~8000 km s^{-1}, which could easily account for the 6000 km s^{-1} (FWZI) width of the absorption lines. However, if the apparent increase in redshift (e.g., between the Hβ profiles of December 8 and 9) were due to an inward displacement of the absorption region, then one would expect an increase in the Keplerian velocity and an increase of ~50% in the FWZI of the lines. No such change is apparent in Figure 5*d*.

4.3. *The Primary Outburst*

An "ultrasoft" spectral component ($kT \sim 1$–2 keV) has until recently been thought a good signature of black hole X-ray novae (e.g., A0620−00, GS 2000+25, Nova Muscae; see Tanaka & Lewin 1995). GRO J0422+32 is only the second black hole X-ray nova (after V404 Cyg) where such a component is conspicuous by its absence. This is clearly evident, for example, in the *MIR Kvant* data of Sunyaev et al. (1993), which were obtained only 20 days after outburst maximum.

A parameter of fundamental interest for X-ray binaries is the ratio of the X-ray to optical luminosity (e.g., van Paradijs & McClintock 1995). For bright LMXBs, the optical and UV luminosity is due to X-ray reprocessing. Here we calculate this ratio for GRO J0422+32 in outburst. We estimate a 2–11 keV flux of 9.3×10^{-9} ergs cm^{-2} s^{-1} at outburst maximum (using the BATSE light curve to scale the *MIR Kvant* data to the time of maximum; see Fig. 2).

Taking a dereddened V magnitude (V_0) at maximum of 12.1, $(B-V)_0 = 0$, and using a UV + optical bolometric correction

TABLE 4A

Equivalent Width of Emission Lines

Date	Hα	Hβ	He II λ4686	He II λ5411	He I λ5876	He I λ6678
1992 Oct 6........	...	−1.7	−2.7	...	...	...
1992 Oct 9	...	−1.2	−2.2	...	...	...
1992 Nov 19......	−2.9	−0.7	−2.0	−1.0	−0.5	−1.2
1992 Nov 21......	−3.6	−0.9	−2.3	−1.0	−0.6	−0.7
1992 Nov 24......	...	−0.8	−2.2	...	...	...
1993 Dec 8	5.8	11.9	...	...	...	...
1993 Dec 9	4.0	6.0	−0.5	...	...	...
1993 Dec 10	−2.6	2.8	−0.9	...	...	−0.2

Note.—Errors on the equivalent width are a few tenths of an angstrom and are dominated by uncertainties in determining the "true" continuum near the broad absorption features.

TABLE 4B

Interstellar Absorption Features (MDM and KPNO Data)

Line	Equivalent Width (Å)
Na D.....................	1.2 ± 0.2
λλ5780, 5788, 5797......	0.5 ± 0.1

of 1.8×10^{-4} ergs cm^{-2} s^{-1} for a $B = 0$ LMXB (van Paradijs 1983a), we estimate a UV + optical flux of 2.8×10^{-9} ergs cm^{-2} s^{-1}. This value is in good agreement with that measured by Shrader et al. (1993) near maximum. From this we infer L_x(2–11 keV)/$L_{\rm bol}$(optical + UV) ~ 4, which is remarkably low compared to the typical value of ~ 50 observed for the persistently bright LMXBs (van Paradijs 1983a). By comparison, for Nova Muscae 1991 we find L_x(2–11 keV)/$L_{\rm bol}$(optical + UV) ~ 75 at maximum (Della Valle et al. 1991a; Kitamoto et al. 1992).

Such a low $L_x/L_{\rm bol}$ ratio has in the past been primarily associated with the high-inclination accretion disk coronae systems (e.g., Mason 1989). However, in the case of GRO J0422+32, the explanation lies instead in the shape of the X-ray spectrum. For a spectrum of photon index 1.5, the ratio of flux in the 10–100/2–10 keV range is ~ 4. Hence the value for $L_x/L_{\rm bol}$ given above is low largely because it ignores the dominant hard component flux. In contrast, the data of Sunyaev et al. (1993) indicate that, for Nova Muscae 1991, the ratio of flux in the 10–100/2–10 keV range is only ~ 0.2. Hence in this case, the ultrasoft component dominates the hard component, and the $L_x/L_{\rm bol}$ ratio is comparable to the persistently bright LMXBs.

4.4. *The Temperature of the Disk*

In Figure 7 we plot the optical flux at outburst against the *GRO* BATSE intensity. As one might expect, the data are strongly correlated. Fitting a power law of the form $F_R = AF_X^{\alpha}$ to the data (where F_R is the R-band flux, and F_X the X-ray 20–300 keV flux measured by BATSE) yields $\alpha = 0.3 \pm 0.05$. Using the technique of Endal, Devinney, & Sofia (1976), we derive a limit on the effective temperature of the accretion disk during outburst of $\geq$28,000 K. This is consistent with that typically observed from X-ray–irradiated disks (van Paradijs 1983a).

4.5. *The Cause of the Minioutbursts*

There are two competing models for the cause of X-ray novae outbursts. In the mass transfer instability (MTI) model the eruption is triggered by irradiation of the secondary star in quiescence (Hameury, King, & Lasota 1986), whereas in the accretion disk instability (ADI) model the eruption is caused by the accretion disk (Mineshige & Wheeler 1989). In the case of cataclysmic variables (CVs) it has proved notoriously difficult to distinguish between the two models. One of the strongest discriminants would be the detection of a gradual increase in magnitude between outbursts—a property predicted by the ADI model but not by the MTI model. Such a systematic brightening has not yet been observed in CVs, although it has been argued that the cooling of the heated white dwarf would reduce the detectability of this effect (e.g., van Amerongen, Kuulkers, & van Paradijs 1990).

We point out here that black hole novae do not suffer from this complication, and that the systematic monitoring of GRO J0422+32 reported here allows us to test this prediction for the minioutbursts. We discuss this further in § 4.5.2, but first we examine in more detail the X-ray and optical characteristics of the minioutbursts.

4.5.1. *The Optical Brightening*

No minioutbursts have previously been detected from any X-ray nova; however, this may well be a selection effect. Our optical monitoring of GRO J0422+32 has been the first thorough study of the return of a X-ray nova to quiescence, and clearly the monitoring of other systems is now warranted.

Although it is clear that the origin of the optical flux at primary outburst is due to X-ray reprocessing in the disk, this is unlikely to be the case for the minioutbursts. Tanaka et al. (1993) report a 0.5–10 keV flux at the maximum of the first minioutburst of 2×10^{-11} ergs cm^{-2} s^{-1} (see Fig. 2). Taking an R magnitude of 14.6 and $A_V = 1$ (see above), and assuming that the slope of the optical spectrum was similar to that in Figure 5*c*, we estimate a dereddened 4000–8100 Å flux of 2×10^{-11} ergs cm^{-2} s^{-1}. For a wide range of blackbody temperatures (4000–30,000 K) the minimum ratio of $L_{\rm bol}/L$(4000–8100 Å) is equal to 2. Hence for GRO J0422+32 during minioutburst $L_x/L_{\rm bol} < 0.5$, even smaller than during primary outburst. If an irradiated disk is to account for the optical flux, and if the irradiating flux is primarily at energies greater than 10 keV (as it appears to be during primary outburst), then the X-ray spectrum during minioutburst must be much harder than during primary outburst (i.e., ≥ 10 times more flux at energies above 10 keV).

However, the slope of the 0.5–10 keV *ASCA* spectrum is no flatter than that observed during primary outburst (Tanaka et al. 1993). Therefore, we conclude that reprocessed X-rays make a small contribution to the optical flux during minioutburst, which is instead dominated by the *intrinsic* luminosity of the

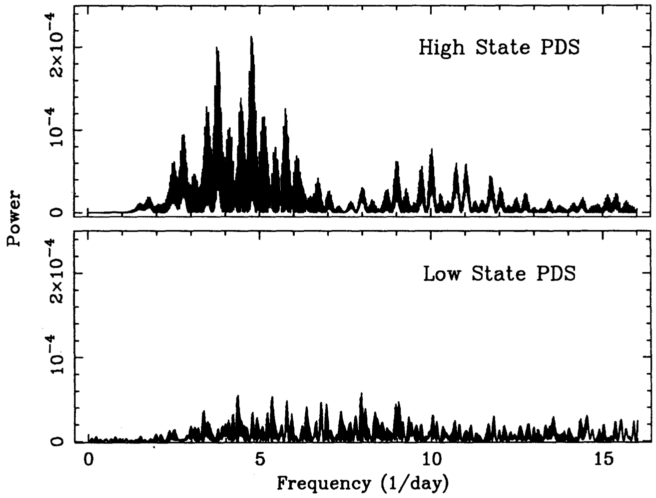

FIG. 6*a*

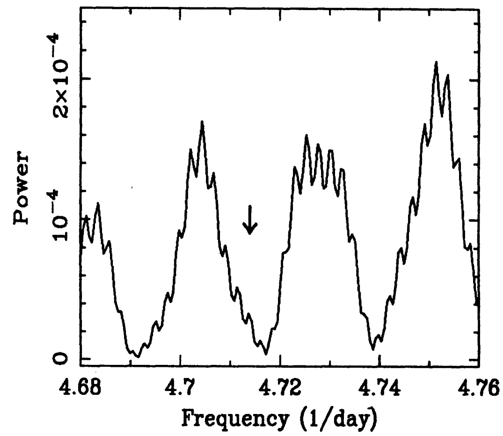

FIG. 6*b*

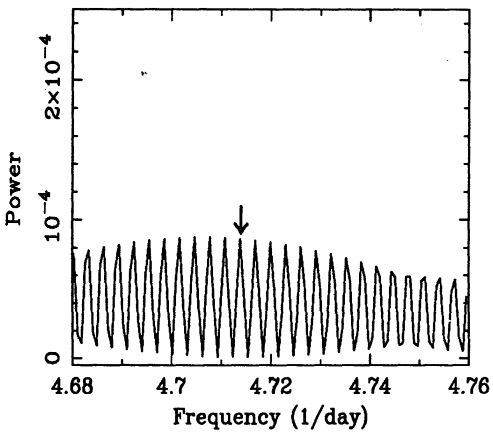

FIG. 6*c*

FIG. 6.—Fourier transforms of the data set presented in Fig. 3. (*a*) Plot of the "high"-state and "low"-state transforms (*upper and lower panels, respectively*); (*b*) expanded plot of the "high"-state Fourier transform; (*c*) plot of the 1993 "high"-state data only.

disk, much like dwarf novae outbursts, in which the X-ray luminosity is a million times less that of X-ray novae, while the accretion disks may be of comparable size.

In this consistent with the estimated absolute magnitude of the minioutburst? We have estimated the M_V(outburst) magnitudes for six dwarf novae from the samples of Ritter (1993) and Berriman (1987), choosing only those systems for which the most accurate distances have been measured. We find M_V(outburst) $= 4.2 \pm 1$ (1 s.d.) mag. Dwarf nova superoutbursts are brighter by ~ 1 mag. For GRO J0422+32, we estimate M_V(minioutburst) = 4 for a distance of 1 kpc. Hence the luminosity of the GRO J0422+32 minioutbursts may be similar to the brighter dwarf nova outbursts, unless the distance to GRO J0422+32 is greater than 3 kpc.

Finally, the 0.2 mag day^{-1} decay timescale of the GRO J0422+32 minioutbursts is comparable to that observed from the longer period dwarf novae: applying the decay time versus orbital period relationship discussed by van Paradijs (1983b), we derive an orbital period of 13.5 ± 2 hr for GRO J0422+32.

4.5.2. *MTI or ADI?*

Our data show no systematic brightening between minioutbursts: in fact, the intensity between minioutbursts actually decreased (see Fig. 2). However, although this is prima facie evidence against the ADI model, it is not conclusive. This is because the extent to which the disk is X-ray–heated, even during interoutburst, is unknown. For example, if the X-ray flux observed by *ASCA* persists through interoutburst, it will have a significant effect on the optical flux of the system near minimum light, rendering the diagnostic discussed in § 4.5 difficult to observe. Unfortunately, no 1–10 keV X-ray measurement during interoutburst has been made to our knowledge, and the BATSE 1 day upper limit, which corresponds to a luminosity of $\sim 10^{36}(d/2\ \mathrm{kpc})^2$ ergs s^{-1} (see § 2.3), does not provide a strong constraint on the models.

Bearing this caveat in mind, we nevertheless favor the MTI X-ray echo model of Augusteijn, Kuulkers, & Shaham (1993), for the following reason. The intervals between the primary BATSE outburst, the BATSE minioutburst (centered approximately at TJD 8980: see Fig. 2), and the subsequent optical minioutbursts are all *multiples of* $\sim$*120 days*. This remarkable quasi-periodicity is a natural consequence of the echo model: mass loss from the secondary is initiated by irradiation from the primary, which leads to additional, quasi-periodic mass loss and quasi-periodic X-ray and optical outbursts.

Note that the X-ray flux detected by *ASCA* during the first optical minioutburst satisfies the criterion for the MTI model. Mineshige et al. (1992) show that the necessary condition for the MTI is $L_x(E > 7\ \mathrm{keV}) > 2.5 \times 10^{34}(M_2/M_\odot)^2$ ergs s^{-1}, where M_2 is the mass of the secondary. Extrapolating the *ASCA* flux at minioutburst to 100 keV, we find that this condition is satisfied if $d/2\ \mathrm{kpc} > (M_2/M_\odot)$. This is consistent with the distance estimate in § 4.1, and with typical masses deduced for secondaries in X-ray novae. However, the irradiation of the secondary is still only a small contribution to the overall optical flux during minioutburst. Hence the modulation we observed during 1993 December cannot be accounted for by a heated secondary, despite its sinusoidal nature. It may instead be due to an SU UMa–like superoutburst periodicity (e.g., Warner 1985).

5. CONCLUSIONS

The unusually protracted decay to quiescence of GRO J0422+32 has been punctuated by at least two minioutbursts of $\sim$4 mag. For much of the time during this decay a 5.1/10.2 hr periodicity has been present in the data; however, this

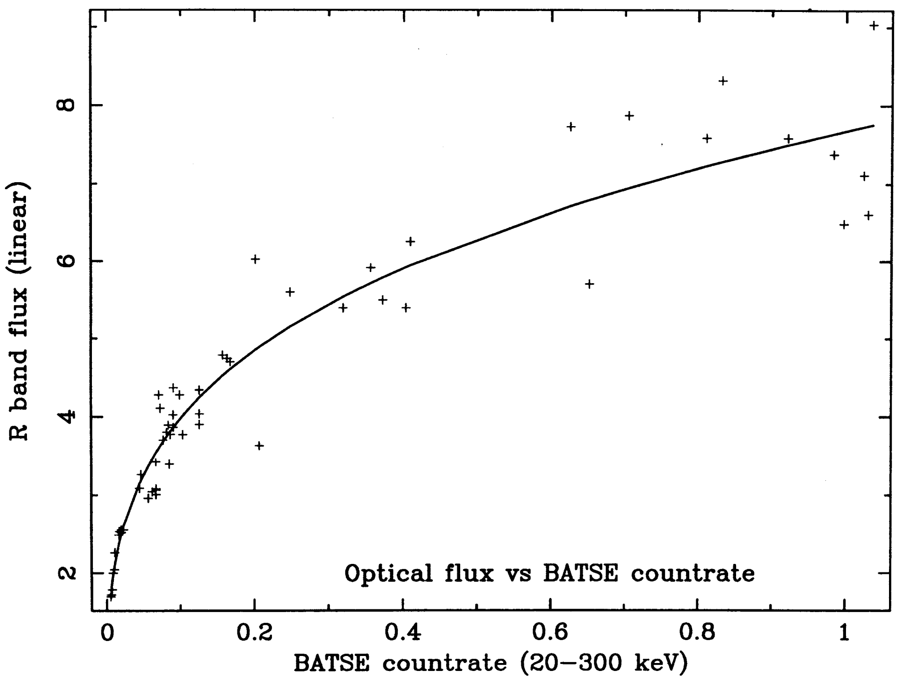

FIG. 7.—*GRO* X-ray and *R*-band optical data, obtained during primary outburst, plotted with the best power-law fit

modulation was conspicuously absent when GRO J0422+32 was in its faintest state (1993 October). Such a periodicity may nevertheless represent the true orbital period; observations when GRO J0422+32 finally reaches its quiescent state are required to confirm this.

Extremely broad (up to 6000 km s^{-1} FWZI) absorption lines have also been observed during both primary outburst and minioutbursts. During minioutbursts these features are redshifted, with double-peaked emission-line cores superposed. These characteristics may point to gross asymmetries in the structure of the accretion disk or a wind.

The interoutburst light curve of GRO J0422+32 may be inconsistent with an accretion disk instability as the origin of the minioutbursts. The low X-ray flux detected by *ASCA* during the first minioutburst precludes X-ray irradiation as the main source of optical flux. The minioutbursts may instead be more akin to the outbursts of dwarf novae. It is clear that systematic long-term monitoring campaigns of other X-ray novae are now sorely warranted.

We thank Jan van Paradijs for useful discussions concerning disk irradiation, and Andy Silber for making his observations of GRO J0422+32 available to us. P. J. C. is supported by NASA through grant HF-1003.01-90A awarded by the Space Telescope Science Institute, and M. R. G. through NASA contract NAS 8-30751.

REFERENCES

Allen, C. W. 1973, Astrophysical Quantities (London: Athlone)
Augusteijn, A., Kuulkers, E., & Shaham, J. 1993, A&A, 279, L13
Barbon, R., Benetti, S., Cappellaro, E., Rosino, L., & Turatto, M. 1990, A&A, 237, 70
Berriman, G. 1987, A&AS, 68, 41
Beskin, G., Neizvestny, S. I., Bartolini, C., Guarnieri, A., & Piccioni, A. 1992, IAU Circ., No. 5610
Bhattacharya, D., & van den Heuvel, E. P. J. 1991, Phys. Rep., 203, 1
Callanan, P. J., & Charles, P. A. 1991, MNRAS, 249, 573
Casares, J., Charles, P. A., & Naylor, T. 1992, Nature, 355, 614
Castro-Tirado, A. J., Pavlenko, E. P., Salyapikov, A. A., Brandt, S., Lund, N., & Ortiz, J. L. 1993, A&A, 276, L37
Charles, P. A., Kidger, M. R., Pavlenko, E. P., Prokofieva, V. V. & Callanan, P. J. 1991, MNRAS, 249, 567
Chevalier, C., & Ilovaisky, S. A. 1992, IAU Circ., No. 5644
Della Valle, M., et al. 1991a, IAU Circ., No. 5165
Della Valle, M., Jarvis, B. J., & West, R. M. 1991b, Nature, 353, 50
Endal, A. S., Devinney, E. J., & Sofia, S. 1976, Astrophys. Lett., 17, 131
Hameury, J. M., King, A. R., & Lasota, J. P. 1986, A&A, 162, 71
Harmon, B. A., et al. 1992, IAU Circ., No. 5584
Harmon, B. A., Zhang, S. N., Wilson, C. A., Rubin, B. C., Fishman, G. J., & Paciesas, W. S. 1993, in The Second Compton Symposium, ed. C. E. Fichtel, N. Gehrels, & J. P. Norris (New York: AIP), 210
Herbig, G. H. 1975, ApJ, 196, 129
Kato, T., Mineshige, S., & Hirata, R. 1993, IAU Circ., No. 5704
———. 1994, submitted to PASJ
Kitamoto, S., Tsunemi, H., Miyamoto, S., & Hayashida, K. 1992, ApJ, 394, 609
Mason K. O. 1989, in Proc. 23d ESLAB Symp., ed. J. Hunt & B. Battrick (ESA SP-296; Paris: ESA), 113
McClintock, J. E., & Remillard, R. A. 1986, ApJ, 308, 110
Mineshige, S., Ebisawa, K., Takizawa, M., Tanaka, Y., Hayashida, K., Kitamoto, S., Miyamoto, S., & Terada, K. 1992, PASJ, 44, 117
Mineshige, S., & Wheeler, J. C. 1989, ApJ, 343, 241
Orosz, J. A., Bailyn, C. D., Remillard, R. A., McClintock, J. E., & Foltz, C. B. 1994, ApJ, 436, 848
Paciesas, W. S., Briggs, M. S., Harmon, B. A., Wilson, R. B., & Finger, M. H. 1992, IAU Circ., No. 5580
Remillard, R. A., McClintock, J. E., & Bailyn, C. 1992, ApJ, 339, L145
Ritter, H. 1993, A&A, 85, 1179
Shrader, C. R., Wagner, R. M., Starrfield, S. G., Hjellming, R. M., & Han, X. H. 1993, in The Second Compton Symposium, ed. C. E. Fichtel, N. Gehrels, & J. P. Norris (New York: AIP), 365
Sunyaev, R. A., et al. 1993, A&A, 280, L1
Tanaka, Y., et al. 1993, IAU Circ., No. 5851
Tanaka, Y., & Lewin, W. H. G. 1995, in X-Ray Binaries, ed. W. H. G. Lewin, J. van Paradijs, & E. P. J. van den Heuvel (Cambridge: Cambridge Univ. Press)
van Amerongen, S., Kuulkers, E., & van Paradijs, J. 1990, MNRAS, 242, 522
van Paradijs, J. 1983a, in Accretion Driven Stellar X-Ray Sources, ed. W. H. G. Lewin & E. P. J. van den Heuvel (Cambridge: Cambridge Univ. Press)
———. 1983b, A&A, 125, L16
van Paradijs, J., & McClintock, J. E. 1995, in X-Ray Binaries, ed. W. H. G. Lewin, J. van Paradijs, & E. P. J. van den Heuvel (Cambridge: Cambridge Univ. Press)
Warner, B. 1976, in Structure and Evolution of Close Binary Systems, ed. P. P. Eggleton, S. Mitton, & J. A. J. Whelan (Boston: Reidel), 85
———. 1985, in Interacting Binaries, ed. P. P. Eggleton & J. E. Pringle (Dordrecht: Reidel), 367
Whelan, J. A. J., et al. 1976, MNRAS, 180, 657
Zhao, P., Callanan, P. J., Garcia, M. R., McClintock, J. E., Remillard, R., & Silber, A. 1994, in AIP Conf. Proc. 308, The Evolution of X-Ray Binaries, ed. S. S. Holt & C. S. Day (New York: AIP), 99